Pseudo-GPS in INS/GPS Loosely-Coupled Integration Approach

Itzik Klein, Sagi Filin, Tomer Toledo

Faculty of Civil Engineering
Technion – Israel Institute of Technology, Haifa 3200, Israel

Published in ATTI Journal of Italian Navigation Institute 190, pp. 35-44, 2009

BIOGRAPHY

Mr. Itzik Klein received the B.Sc and M.Sc degrees in Aerospace Engineering from the Technion - Israel Institute of Technology, in 2004 and 2006 respectively. Since 2007 he is studying towards Ph.D. degree in Geodetic and Transportation Engineering at the Technion - Israel Institute of Technology.

Dr. Sagi Filin received the B.Sc and M.Sc degrees in Geodetic Engineering from the Technion - Israel Institute of Technology, in 1989 and 1995 respectively. In 2001 he received the Ph.D. degree in Geodetic Sciences from The Ohio State University. From 2001 until 2004 he was with the Photogrammetry and Remote Sensing Section in Delft University of Technology. Since 2004 he is a faculty member in Civil and Environmental Engineering in the Department of Transportation and Geo-Information Engineering.

Dr. Tomer Toledo is a Senior Lecturer at the Transportation Research Institute and Faculty of Civil and Environmental Engineering at the Technion – Israel Institute of Technology in Haifa Israel. He received a Ph.D. in Transportation Systems from the Massachusetts Institute of Technology in 2002. Dr. Toledo's research is in the areas of large-scale traffic simulation, driver behavior and safety, and intelligent transportation systems.

1. INTRODUCTION

The integration of GPS and INS is aim at utilizing the advantages of each system and to compromise their weakness. Four types of GPS/INS coupling architectures have been proposed: 1. uncoupled, 2. loosely coupled, 3. tightly coupled and 4. ultra-tightly (deep) coupled.

In the uncoupled integration architecture [1], the GPS estimated position and velocity are used to reseat the INS indicated position and velocity at regular intervals of time. Although, this approach involves minimal changes to either systems, it does not provide the opportunities for performance enhancement and jamming avoidance. In addition, when GPS is not available, system accuracy decreases rapidly.

The loosely coupled integration approach [2] allows the GPS to function autonomously and simultaneously enables INS and GPS integrated solution. In the integrated solution, INS and GPS estimates of position and velocity are compared and the resulting differences form the measurement inputs to the estimation filter. The advantage of the loosely coupled approach lies in its redundancy since two navigation solutions are given to the user: 1. a standalone GPS solution and 2. an integrated INS/GPS solution. In addition, this integration approach is suitable for any INS and GPS receiver, and can be used to retro-fit applications [1]. On the other hand, four GPS satellites are required to form a GPS solution. So, unless four or more satellites are available, the loosely coupled approach relies on the INS standalone solution which, regardless to its grade, will drift in time [3].

Another INS/GPS integration approach is the tightly coupled approach. In this approach, there is no separated GPS navigation solution. A single integration filter is employed to fuse INS and GPS measurements [4]. The raw pseudorange and pseudorate measurements from the GPS output and those constructed from the INS prediction are combined to form the measurement to the estimation filter. The filter directly accepts their differences to obtain the INS error estimates [5].

This scheme provides a more accurate solution than the loose integration because the basic GPS observables (pseudorange and pseudorate) used in the blending process are not as correlated as the position and velocity solutions (used in loosely coupled approach) are [6].

The final INS/GPS integration approach is the ultra tight integration. This integration scheme combines GPS signal tracking and INS-GPS integration into a single estimation filter. Conceptually, in this approach INS is aiding the GPS while in the other integration schemes GPS is aiding the INS. Although this integration approach has several advantages such as: faster GPS signal reacquisition and multipath resistance is improvement [1], it can only be realized in a special hardware component and requires access to the firmware of the receiver [5].

The loosely coupled integration system has both advantages and disadvantages compared to the tightly coupled one [7], [8]. In the aspect of system implementation, the loosely coupled integration system has higher flexibility and modularity as well as less computation and complexity due to the independent operation and the smaller dimensions of the individual Kalman filter. In terms of system accuracy, the tightly coupled integration system provides a globally optimal estimation-accuracy, because all the states for the entire system are defined in one global state-vector with a corresponding global description of the process noise. In terms of system availability, the loosely coupled integration system requires at least four GPS satellites to provide GPS updates for INS corrections while the tightly coupled method can still operate with as few as one GPS satellite. For system robustness, the loosely coupled integration system has higher fault detection performance than the tightly coupled one because the independent filter solutions are available from two separate filters.

In this paper we propose constructing artificial GPS measurements to facilitate GPS receiver position and velocity solutions in situations were less than four satellites are available, and thus enabling the implementation of the loosely coupled integration approach. The pseudo-GPS measurements are constructed in the following manner: from the last almanac message the location and velocity of all GPS satellites can be propagated by time and thus considered/become known. In addition, from the INS, the user position and velocity is estimated. Combining both INS position and velocity with the pseudo-GPS satellites position and velocity, the artificial pseudoranges and pseudorates can be calculated for satellites which are not viewed by the GPS receiver. These pseudoranges and pseudorates are used to calculate the GPS receiver position and velocity, which are introduced to the estimation process.

Since pseudo-GPS measurements are used, any GPS satellite can be chosen from the GPS constellation. Therefore, extra pseudo-GPS measurements can be added to enhance the position and velocity solution. Additionally, appropriate satellites can be chosen to minimize the Dilution of Precision (DOP) of the satellites.

We demonstrate the usefulness of the proposed method through several illustrative examples. In those examples we use MEMES INS data collected in field experiments. In all examples, the introduction of pseudo-GPS measurements greatly reduced the navigation errors obtained with the standalone INS.

The paper is organized as follows: Section 2 introduces the fundamental principles in which this paper is based upon. Section 3 describes the concept of pseudo-GPS while in Section 4 some illustrative examples are presented. The conclusions of this research are discussed in section 5.

2. GPS/INS LOOSELY COUPLED APPROACH

2.1 INS ERROR EQUATIONS

The following coordinate frames are used in this work: Inertial frame (i-frame), Earth Centered Earth Fixed (e-frame) frame, North-East-Down (NED) frame (n-frame) and Body frame (b-frame). The i-frame origin is at the center of the Earth. The x-axis points towards the mean Vernal equinox, the z-axis is parallel to the Earth spin axis and the y-axis completes a right handed orthogonal frame. The e-frame has its origin at the center of the Earth and rotates with the Earth spin. The x-axis points towards the Greenwich meridian, the z-axis is parallel to the Earth spin axis and the y-axis completes a right handed orthogonal frame. The n-frame has its origin fixed on the earth surface at the initial latitude/longitude of the vehicle. The x-axis points towards the geodetic north, the z-axis is on the local vertical pointing down and the y-axis completes a right handed orthogonal frame. The b-frame origin is at the vehicle center of mass. The x-axis is parallel to the vehicle longitudinal symmetry axis pointing forward, the z-axis points down and the y-axis completes a right handed orthogonal frame.

Raw measurements from accelerometers and gyros are measured along the b-frame. They are

transformed to the n-frame, where data integration is performed. The position in the n-frame is expressed by curvilinear coordinates $r^n = \begin{bmatrix} \phi & \lambda & h \end{bmatrix}^T$ where, ϕ is the latitude, λ is the longitude and h is the height above the Earth surface. The equations of motion in the n-frame are given by [1]:

$$\begin{bmatrix} \dot{r}^n \\ \dot{v}^n \\ \dot{T}^{b\to n} \end{bmatrix} = \begin{bmatrix} D^{-1}v^n \\ T^{b\to n}f^b + g_1^n - \left(2\omega_{ie}^n + \omega_{en}^n\right)\times v^n \\ T^{b\to n}\Omega_{nb}^b \end{bmatrix} \quad (1)$$

$$D^{-1} = \begin{bmatrix} \frac{1}{(M+h)} & 0 & 0 \\ 0 & \frac{1}{(N+h)\cos(\phi)} & 0 \\ 0 & 0 & -1 \end{bmatrix} \quad (2)$$

where $v^n = \begin{bmatrix} v_N & v_E & v_D \end{bmatrix}$ is the vehicle velocity, $T^{b\to n}$ and $T^{n\to b}$ are the transformation matrices from the b-frame to the n-frame and vice-versa, respectively. f^b is the measured specific force, ω_{ie}^n is the Earth rate with respect to the i-frame, ω_{en}^n is the turn rate of the n-frame with respect to the Earth, g_1^n is local gravity vector, *M* and *N* are the radii of curvature in the meridian and prime vertical, respectively and Ω_{nb}^b is the skew-symmetric form of the body rate with respect to the n-frame given by:

$$\omega_{nb}^b = \omega_{ib}^b - T^{n\to b}\left(\omega_{ie}^n + \omega_{en}^n\right) \quad (3)$$

The INS mechanization equations provide no information about errors in the system states (caused by measurement errors) as they process raw data from the Inertial Measurement Unit (IMU) to estimate navigation parameters. The IMU outputs contain additional errors that cannot be compensated for. These errors are due to uncertainties in the sensors such as spurious magnetic fields and temperature gradients. Thus, to improve the performance of the INS it is necessary to develop an error model which describes how the IMU sensor errors propagate through the equation of motion (Eq. (1)) into navigation errors. These navigation errors are then corrected for in order to obtain corrected navigation solution.

Several models (e.g. [9], and [1]) were developed to describe the time-dependent behavior of these errors. A classic approach is the perturbation analysis, in which navigation parameters are perturbed with respect to the true n-frame. This is done by taking a first order Taylor series expansion of the states in Eq. (1). A complete derivation of this model can be found for example in [10], and [11]. The state-space model is given by:

$$\begin{bmatrix} \delta\dot{r}^n \\ \delta\dot{v}^n \\ \dot{\varepsilon}^n \\ \delta\dot{b}_a \\ \delta\dot{b}_g \end{bmatrix} = F\begin{bmatrix} \delta r^n \\ \delta v^n \\ \varepsilon^n \\ \delta b_a \\ \delta b_g \end{bmatrix} + G\begin{bmatrix} \upsilon_a \\ \upsilon_g \\ \upsilon_{ba} \\ \upsilon_{bg} \end{bmatrix} \quad (4)$$

$$F = \begin{bmatrix} F_{rr} & F_{rv} & 0_{3\times3} & 0_{3\times3} & 0_{3\times3} \\ F_{rv} & F_{vv} & f^n & T^{b\to n} & 0_{3\times3} \\ F_{er} & F_{ev} & -\Omega_{in}^n & 0_{3\times3} & -T^{b\to n} \\ 0_{3\times3} & 0_{3\times3} & 0_{3\times3} & \left(-1/\tau_a\right)_{3\times3} & 0_{3\times3} \\ 0_{3\times3} & 0_{3\times3} & 0_{3\times3} & 0_{3\times3} & \left(-1/\tau_g\right)_{3\times3} \end{bmatrix} \quad (5)$$

$$G = \begin{bmatrix} 0_{3\times3} & 0_{3\times3} & 0_{3\times3} & 0_{3\times3} \\ T^{b\to n} & 0_{3\times3} & 0_{3\times3} & 0_{3\times3} \\ 0_{3\times3} & -T^{b\to n} & 0_{3\times3} & 0_{3\times3} \\ 0_{3\times3} & 0_{3\times3} & I_{3\times3} & 0_{3\times3} \\ 0_{3\times3} & 0_{3\times3} & 0_{3\times3} & I_{3\times3} \end{bmatrix} \quad (6)$$

where the state vector consists of position error, velocity and attitude errors and accelerometer and gyro bias/drift. A detailed description of the parameters in Eq. (4) is given in an appendix. Eq. (4) defines the system dynamics for the linear Kalman filter, which is introduced in the next section.

2.2. GPS POSITION AND VELOCITY CALCULATIONS

The standard GPS positioning problem involves four unknown quantities: the receiver position vector in the e-frame $\begin{bmatrix} x_p & y_p & z_p \end{bmatrix}$ and the receiver clock bias Δt_r. Those quantities can be obtained by solving the following measurement equation for four satellites

$$\tilde{\rho}_i = \left[\left(X_i - x_p\right)^2 + \left(Y_i - y_p\right)^2 + \left(Z_i - z_p\right)^2\right]^{\frac{1}{2}} + c\Delta t_r \quad (7)$$

where $\tilde{\rho}_i$ is the measured pseudorange of the i-th satellite, $\begin{bmatrix} X_i & Y_i & Z_i \end{bmatrix}$ is the i-th satellite e-frame

position vector and c is the speed of light. Let, $x = \begin{bmatrix} x_p & y_p & z_p & c\Delta t_r \end{bmatrix}^T$ then the objective of the solution will be to find the value of x that minimizes the cost function [12]

$$J(\hat{x}) = \left\| \hat{\rho}(\hat{x}) - \tilde{\rho} \right\| \tag{8}$$

where $\tilde{\rho}$ is a set of at least four pseudorange measurements and $\hat{\rho}(\hat{x})$ is the set of the computed pseudorange which are a function of the computed satellites position. The algorithm which finds the value of $\hat{x}$ that minimizes the cost function (8) is given by

$$\hat{x}_{k+1} = \hat{x}_k + \left(H^T H \right)^{-1} H^T \left[\tilde{\rho} - \hat{\rho}(\hat{x}) \right] \tag{9}$$

where

$$H = \begin{bmatrix} \frac{\delta\rho_1}{\delta x} & \frac{\delta\rho_1}{\delta y} & \frac{\delta\rho_1}{\delta z} & 1 \\ \frac{\delta\rho_2}{\delta x} & \frac{\delta\rho_2}{\delta y} & \frac{\delta\rho_2}{\delta z} & 1 \\ \frac{\delta\rho_3}{\delta x} & \frac{\delta\rho_3}{\delta y} & \frac{\delta\rho_3}{\delta z} & 1 \\ \frac{\delta\rho_4}{\delta x} & \frac{\delta\rho_4}{\delta y} & \frac{\delta\rho_4}{\delta z} & 1 \end{bmatrix} \tag{10}$$

$$\frac{\delta\rho_i}{\delta x} = \frac{-\left(X_i - x\right)}{\left[\left(X_i - x\right)^2 + \left(Y_i - y\right)^2 + \left(Z_i - z\right)^2 \right]^{\frac{1}{2}}}$$

$$\frac{\delta\rho_i}{\delta y} = \frac{-\left(Y_i - y\right)}{\left[\left(X_i - x\right)^2 + \left(Y_i - y\right)^2 + \left(Z_i - z\right)^2 \right]^{\frac{1}{2}}} \tag{11}$$

$$\frac{\delta\rho_i}{\delta z} = \frac{-\left(Z_i - z\right)}{\left[\left(X_i - x\right)^2 + \left(Y_i - y\right)^2 + \left(Z_i - z\right)^2 \right]^{\frac{1}{2}}}$$

The iteration of Eq. (9) is performed until $\left(H^T H \right)^{-1} H^T \left[\tilde{\rho} - \hat{\rho}(\hat{x}) \right]$ had a magnitude less than a prespecified threshold.

In the same manner the receiver velocity, $\hat{v}$, is being calculated. Let $v = \begin{bmatrix} v_{xp} & v_{yp} & v_{zp} & c\Delta\dot{t}_r \end{bmatrix}^T$, then [4]

$$\hat{v}_{k+1} = \hat{v}_k + \left(H^T H \right)^{-1} H^T \left[\tilde{d} - \hat{d}(\hat{v}) \right] \tag{12}$$

where H is defined in Eq. (10) and

$$\tilde{d}_i = \left[v_{xp} \frac{\left(X_i - x_p\right)}{r_i} + v_{yp} \frac{\left(Y_i - y_p\right)}{r_i} + v_{zp} \frac{\left(Z_i - z_p\right)}{r_i} \right] + c\Delta\dot{t}_r \tag{13}$$

$$r_i = \left[\left(X_i - x_p\right)^2 + \left(Y_i - y_p\right)^2 + \left(Z_i - z_p\right)^2 \right]^{\frac{1}{2}} \tag{14}$$

2.3 LINEAR KALMAN FILTER

We incorporate the INS dynamics with the GPS position and velocity measurements in a linear Kalman filter. In general, a Kalman filter algorithm consists of two steps: prediction of the state based on the system model, and update of the state based on the measurements. The first step in the Kalman filter is prediction of the state and its associated covariance [13]:

$$\hat{x}_{k+1}^- = \Phi \hat{x}_k^+ , \Phi = e^{F(t)\Delta t} \tag{15}$$

$$P_{k+1}^- = \Phi P_k^+ \Phi^T + Q_k \tag{16}$$

where the superscripts – and + represent the predicted quantity (before measurement update) and the updated quantity (after measurement update). x and P are the system state and the associated error covariance matrix, respectively. Φ is the state transition matrix from time *k* to time *k+1*, $F(t)$ is the system dynamics matrix and Q_k is the process noise covariance matrix [14] given by:

$$Q_k \approx \frac{1}{2} \left[\Phi_k G(t_k) Q(t_k) G^T(t_k) + G(t_k) Q(t_k) G^T(t_k) \Phi_k^T \right] \Delta t \tag{17}$$

where, $G(t)$ is the shaping matrix. Δt is the time step. The second step is the measurement update:

$$K_{k+1} = P_{k+1}^- H_{k+1}^T \left(H_{k+1} P_{k+1}^- H_{k+1}^T + R_{k+1} \right)^{-1} \tag{18}$$

$$\hat{x}_{k+1}^+ = \hat{x}_{k+1}^- + K_{k+1} \left(z_{k+1} - H_{k+1} \hat{x}_{k+1}^- \right) \tag{19}$$

$$P_{k+1}^+ = \left(I - K_{k+1} H_{k+1} \right) P_{k+1}^- \tag{20}$$

where K_k is the Kalman gain, H_k is the measurement matrix, R_k is the measurement noise covariance matrix and z_k is the measurement.

Let $x_{KF} = \begin{bmatrix} \delta r^n & \delta v^n & \varepsilon^n & \delta b_a & \delta b_g \end{bmatrix}^T$ be the state vector, thus the system dynamics and shaping matrices are defined in Eqs. (4)-(6) which can be written in the following manner

$$\dot{x}_{KF} = Fx_{KF} + Gu \tag{21}$$

In the loosely coupled integration approach position and velocity from the GPS are inserted as measurements to the Kalman filter which uses it to estimate the INS errors states. The measurement equation is given by

$$z_{LC} = \begin{bmatrix} r_{INS} - r_{GPS} \\ v_{INS} - v_{GPS} \end{bmatrix} \tag{22}$$

where r_{INS} and v_{INS} are, respectively ,the INS position and velocity solution and r_{GPS} and v_{GPS} are the GPS position and velocity solution, respectively. The corresponding measurement matrix is given by

$$H_{LC} = \begin{bmatrix} I_3 & 0_3 & 0_3 & 0_3 & 0_3 \\ 0_3 & I_3 & 0_3 & 0_3 & 0_3 \end{bmatrix} \tag{23}$$

As noted in the introduction, the two main advantages of the loosely coupled integration approach are simplicity and redundancy. However, when less than four satellites are accessible, no GPS position and velocity solution is available, disabling usage of the loosely coupled approach. In the next section we introduce the pseudo-GPS approach which enables the usage of loosely coupled approach even with less than four accessible satellites.

3. PSEUDO-GPS

3. PSEUDO-GPS METHODOLOGY

In order to obtain receiver position and velocity, four GPS satellites are required. In the loosely coupled approach, when less than four satellites are available, the navigation solution depends only on the standalone INS solution. Therefore, the navigation solution will drift in time. The drift rate depends on the quality of the employed INS. Yet, high quality INS is much expensive compared to MEMS INS. In the pseudo-GPS methodology we propose creating pseudo-GPS satellites when less than four satellites are available based on the position and velocity obtained from a MEMS INS. The pseudo-GPS satellites are then taken together with the true satellites, viewed by the receiver, to form at least four satellites. This way, receiver GPS position and velocity can be obtained with even less than four actual satellites, enabling the usage of the loosely coupled approach.

Let $n < 4$ satellites acquired by the receiver, then $m = 4 - n$ pseudo-GPS satellites are to be created. We create the pseudo-GPS satellites in the following manner: from the almanac, position and velocity of each GPS satellite can be calculated at the beginning of each week. Those position and velocity can be propagated by Kepler motion equations [15]:

$$\ddot{r} + \frac{\mu r}{\|r\|^3} = p(r,t) \tag{24}$$

where μ is the gravitational parameter and $p(r,t)$ denotes the perturbations acting upon the satellite. For simplicity we neglect all perturbations on the satellites orbit, including the perturbing acceleration due to the zonal harmonics J_2 by setting $p(r,t) = 0$. In that manner, we can produce GPS orbits which resembles to the true ones. The accuracy of the orbit depends on the employed integrator and the proximity to the almanac time of update. In addition to the GPS satellite position and velocity obtained from Eq. (24), the INS position and velocity are known in each moment. Thus, we can calculate the pseudo-GPS pseudorange and rate by

$$\tilde{\rho}_{P-GPS} = \left[(X_i - x_{INS})^2 + (Y_i - y_{INS})^2 + (Z_i - z_{INS})^2 \right]^{\frac{1}{2}} \tag{25}$$

$$\dot{\tilde{\rho}}_{P-GPS} = \frac{\left[(X_i - x_{INS})(V_{xi} - v_{xINS}) + (Y_i - y_{INS})(V_{yi} - v_{yINS}) + (Z_i - z_{INS})(V_{zi} - v_{zINS}) \right]}{\tilde{\rho}_{P-GPS}} \tag{26}$$

Once the pseudo-GPS pseudorange and rate are obtained from Eqs. (25)-(26), they are combined with the true measured pseudorange and rate and with the true and pseudo-GPS satellites positions and velocities and substituted into Eqs. (9)-(14) to obtain GPS position and velocity. Then, GPS position and velocity are introduced into Eq. (22) as aiding to the INS estimation process. This pseudo-GPS methodology is presented in terms of a flowchart in Figure 1.

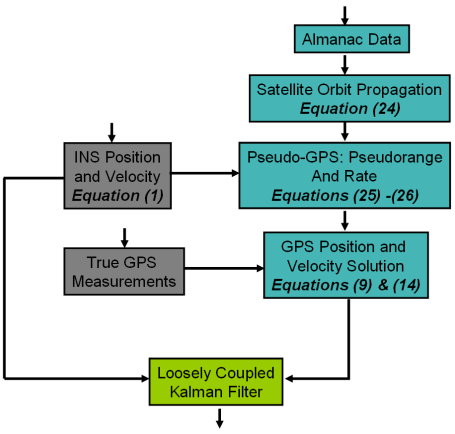

Figure 1: Pseudo-GPS Methodology

4 ANALYSIS & DISCUSSION

The pervious section demonstrated how pseudo-GPS satellites can be created, while this section discusses which satellites to choose from the existing GPS constellation as pseudo-GPS satellites. In addition, the effect of the number of pseudo-GPS satellites employed on the navigation solution is examined.

Firstly, since we construct the pseudo-GPS satellites any satellite from the existing GPS constellation can be chosen. More specifically, we examine three approaches: 1. Add arbitrary satellites from the GPS constellation to form at least four satellites (arbitrary satellites approach) 2. Add arbitrary satellites from the GPS constellation to form more than four satellites (extra satellites approach) 3. Choose appropriate satellites from the GPS constellation in order to minimize the Dilution of Precision (DOP) of the viewed satellites (minimizing DOP approach). The DOP is a quality measure for the geometry of the viewed GPS satellites, and is directly related to the accuracy of the GPS solution. Loosely speaking, an error in the GPS solution is estimated by the pseudorange error factor multiplied by the satellite geometry factor (DOP). The pseudorange error factor is the User Equivalent Range Error (UERE), which contains all error sources (Ionosphere, multipath, etc.).

The lowest value of the DOP is one, representing ideal conditions, while the highest value of the DOP is 50 representing poor conditions. It was shown [16] that the configuration to yield minimum DOP is tetrahedron with an equilateral triangle as its base. That is, one satellite at the zenith of the user and other satellites equally spaced in a plane perpendicular to the user link to the satellite zenith. Therefore, when less than four satellites are in view, we can calculate which pseudo-satellites to create to minimize the DOP.

Let $n < 4$ satellites be acquired by the receiver, then at least $m = 4 - n$ pseudo-GPS satellites are to be created in order to obtain GPS position and velocity solution. Thus, for each of the above mentioned approaches we have

1. Arbitrary Satellites: a set of m satellites are chosen from the GPS constellation and their corresponding pseudorange and rate are constructed.
2. Extra Satellites: a set of $m^* > m$ satellites are chosen from the GPS constellation and their corresponding pseudorange and rate are constructed.
3. Minimizing DOP: a set of m appropriate satellites which together with the viewed satellites yield the minimum DOP are chosen from the GPS constellation and their corresponding pseudorange and rate are constructed.

To demonstrate the usefulness of the proposed pseudo-GPS approaches, an example featuring data collected using MEMS INS while driving in an urban environment is presented. For the nominal trajectory we used the GPS solution of the corresponding INS trajectory. The nominal trajectory has a height variation of about 15 meters and includes left/right turning. The car velocity was changing in this scenario but did not exceed 70 km/h. Raw data was collected over 60 seconds. One hundred Monte-Carlo trials were made to examine if the choice of the arbitrary satellites has any influence on the navigation solution. At the start of each individual trial an arbitrary set of pseudo-GPS satellites was chosen. The appropriate satellites to yield the best DOP were found at the beginning of each trial and were used throughout. Even though it is possible to perform this calculation in each time-step or after a desired period, in this work we chose performing it only at the starting point of the case-study.

To evaluate the contribution of the pseudo-GPS approach, the following error measure is utilized:

$$\varepsilon_x(t) = x_{aiding}(t) - x_{nominal}(t) \qquad (27)$$

where $\varepsilon_x(t)$ is the error for state x, $x_{aiding}(t)$ is the state history obtained from the pseudo-GPS aiding and $x_{nominal}(t)$ is the nominal state history.

First, to evaluate the proposed method we nullify all GPS related noises (i.e., measurement noise clock bias, etc.) and assume the pseudo-GPS orbits are known precisely. Therefore, the only noise included in the pseudorange and pseudorate calculations (Eqs. (25)-(26)), is hidden in the INS position and velocity. The results for this case study are shown in Figures 2-7.

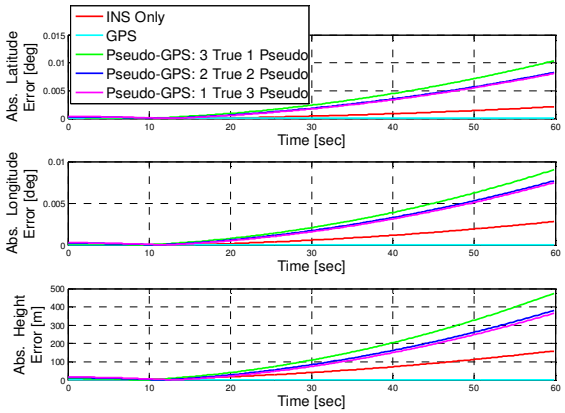

Figure 2: Position error for arbitrary satellites

Figures 2-3 address the case of adding an arbitrary set of satellites from the GPS constellation to complete for four true and pseudo satellites. As can be seen in Figure 2, all position vector components error received poor results compared with the standalone INS. However, each of the errors in the velocity components was reduced by ~50% compared to the standalone INS, but the velocity components still drift with time.

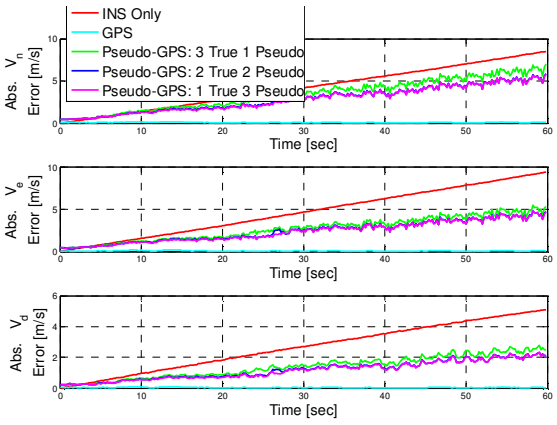

Figure 3: Velocity error for arbitrary satellites

The performance of the arbitrary satellites approach can be improved by replacing the arbitrary set of satellites with an appropriate set which minimizes the DOP. Results of this approach are presented in Figures 4-5.

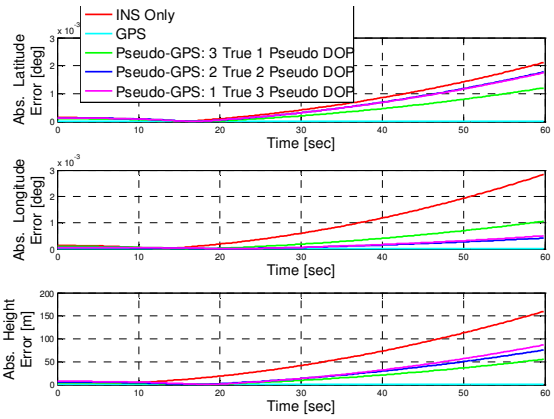

Figure 4: Position error for minimizing DOP satellites

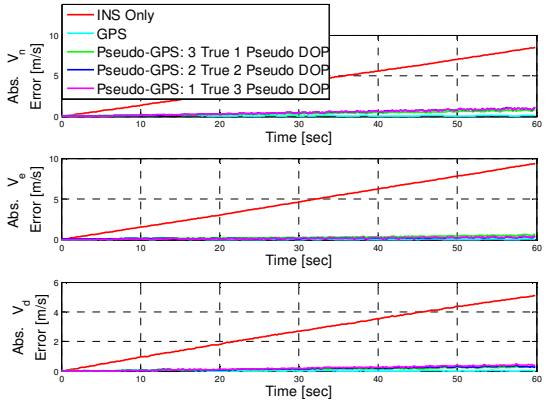

Figure 5: Velocity error for minimizing DOP satellites

As Figure 4 shows, using this approach the error in the position is lower than the standalone INS solution; however it still drifts with time. Figure 5 shows however that the error in the velocity components is bounded for the studied period. Additionally, errors at the end of the experiment were reduced by an order-of-magnitude compared to the standalone INS. This result is obtained regardless to the number of viewed GPS satellites: one, two or three.

Figures 6-7 show a comparison between the three pseudo-GPS approaches for the position and velocity error.

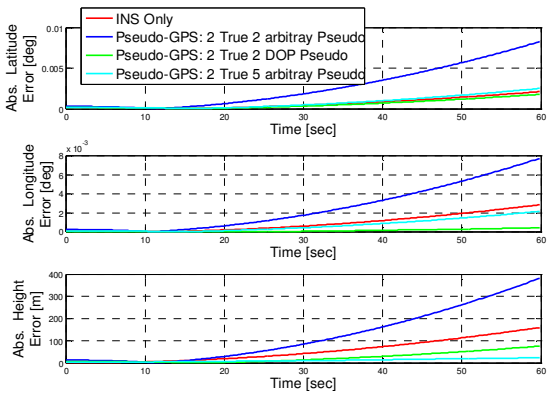

Figure 6: Comparison between the three pseudo-GPS approaches for the position error

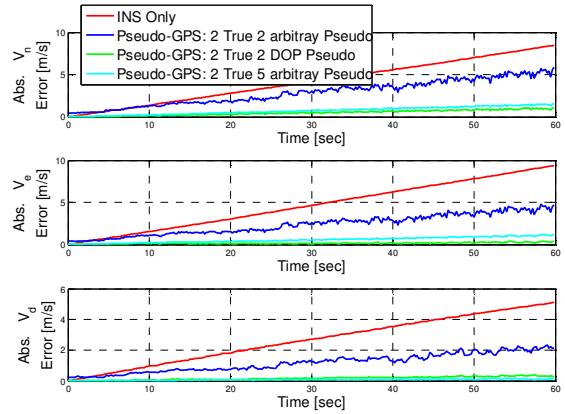

Figure 7: Comparison between the three pseudo-GPS approaches for the velocity error

As can be seen from Figures 6-7, adding an arbitrary set of extra satellites improved the performance of completing to four satellites but error was much higher compared to the DOP minimization driven approach. Therefore, adding pseudo-satellites to complete for four satellites showed less improvement relative to the standalone INS while choosing appropriate DOP satellites had mange to bound all three velocity components error.

To further evaluate the proposed method, GPS related noises (i.e., measurement noise clock bias, etc.) are inserted to the GPS measurements and a drift error is introduced to the pseudo-GPS orbits. The results for this case study are shown in Figures 8-9. As can be seen, an introduction of noises did not influence the overall results. When comparing the position error, the arbitrary satellites approach had poorer results compared to the standalone INS. Although the minimizing DOP approach had improved the standalone INS error, its error is not bounded. On the other hand, all three approaches, regardless to the number of pseudo satellites used show great improvement relative to the standalone INS when comparing the velocity errors.

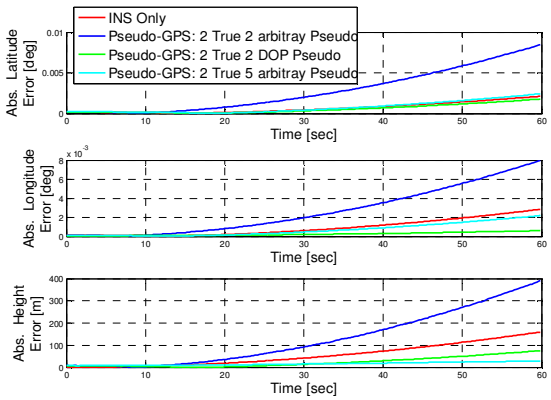

Figure 8: Comparison between the three pseudo-GPS approaches for the position error with noises

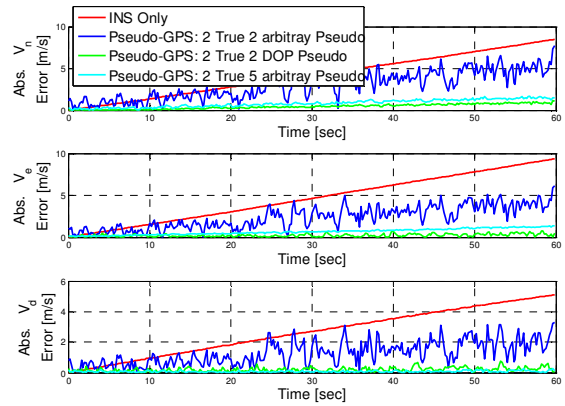

Figure 9: Comparison between the three pseudo-GPS approaches for the velocity error with noises

5. CONCLUSIONS

This paper proposed constructing pseudo GPS measurements in order to facilitate GPS receiver position and velocity solutions in situations where less than four satellites are available and thus enabling the implementation of the loosely coupled integration approach. We demonstrated three approaches for the pseudo-GPS method: 1. adding an arbitrary set satellites from the GPS constellation to form at least four satellites 2. adding an extra set of arbitrary satellites from the GPS constellation to form more than four satellites 3. choosing satellites from the GPS constellation for minimizing the DOP.

Results show that all three approaches and regardless to the number of pseudo-GPS satellites

used, greatly improved the standalone INS performance when comparing the error in the velocity components. In particular minimizing DOP approach yielded bounded error in the velocity components. The analysis shows that pseudo-GPS method performance is degraded over time since the INS position and velocity drifts with time, but this could be compensated for by using a better-grade INS.

The proposed model requires no hardware change, and only the addition of the pseudo-GPS algorithm to the software. With this small modification the loosely coupled approach can be implemented even with one available satellite.

6. REFERENCES

[1] D. H. Titterton and J. L. Weston, Strapdown inertial navigation technology – second edition, The American Institute of Aeronautics and Astronautics and the institution of electrical engineers, 2004.

[2] M. S. Grewal, L. R. Weill and A. P. Andrews, Global positioning systems, inertial navigation and integration second edition, John Wiley & Sons, INC., Publications, 2007.

[3] J. A. Farrell and M. Barth, The global positioning system & inertial navigation, McGraw-Hill, 1999

[4] E. D. Kaplan and C. J. Hegarty, Understanding GPS principles and applications second edition, Artech House, 2006.

[5] K-W. Chiang, INS/GPS integration using neural networks for land vehicular navigation applications, Dissertation thesis – department of geomatics and engineering , Calgary, Alberta, Canada, 2004.

[6] S. Alban, D. Akos, S. Rock and D. Gebre-Egziabher, Performance analysis and architectures for INS-aided GPS tracking loops, Proceedings of the Institute of Navigation National Technical Meeting, 2003.

[7] S. Godha, Performance evaluation of low cost MEMS-based IMU integrated with GPS for land vehicle navigation application, A thesis – department of geomatics and engineering , Calgary, Alberta, Canada, 2006.

[8] P. D. Groves, Principles of GNSS, inertial and multisensor integrated navigation systems, Artech House, 2008

[9] C. Jekeli, inertial navigation systems with geodetic applications, Walter de Gruyter Berlin, Germany, 2000.

[10] P. G. Savage, Strapdown analytics: Part 1, Strapdown Associates Inc., Maple Plain, Minnesota, 2000.

[11] E.-H. Shin, Estimation techniques for low-cost inertial navigation, UCGE reports number 20219, the University of Calgary, Calgary, Alberta, Canada, 2005.

[12] J. A. Farrell, Aided navigation GPS with high rate sensors, McGraw-Hill, 2008.

[13] P. Zarchan and H. Musoff, Fundamentals of Kalman filtering: a practical approach second edition, The American Institute of Aeronautics and Astronautics, 2005.

[14] Maybeck P. S., Stochastic models, estimation and control, Volume 1, Navtech Book & Software store, 1994.

[15] R. H. Battin, An introduction to the mathematics and methods of astrodynamics, The American Institute of Aeronautics and Astronautics, 1999.

[16] B. W. Parkinson and J. J. Spiker Jr., Global Positioning System: theory and applications, Volume I, American Institute of Aeronautics and Astronautics, 1996.

7. APPENDIX

The following matrixes are associated with the INS state space error model Eq. (4)

$$F_{rr} = \begin{bmatrix} 0 & 0 & \dfrac{-V_N}{(M+h)^2} \\ \dfrac{V_E \sin(\phi)}{(N+h)\cos^2(\phi)} & 0 & \dfrac{-V_E \sin(\phi)}{(N+h)^2 \cos^2(\phi)} \\ 0 & 0 & 0 \end{bmatrix} \quad \text{(A.1)}$$

$$F_{rv} = \begin{bmatrix} \dfrac{1}{(M+h)} & 0 & 0 \\ 0 & \dfrac{1}{(N+h)\cos(\phi)} & 0 \\ 0 & 0 & -1 \end{bmatrix} \quad \text{(A.2)}$$

$$F_{vr} = \begin{bmatrix} -2V_E\omega_e \cos(\phi) - \dfrac{V_E^2}{(N+h)\cos^2(\phi)} & 0 & \dfrac{-V_N V_D}{(M+h)^2} + \dfrac{V_E^2 \tan(\phi)}{(N+h)^2} \\ 2\omega_e\left(V_N \cos(\phi) - V_D \sin(\phi)\right) + \dfrac{V_E V_N}{(N+h)\cos^2(\phi)} & 0 & \dfrac{-V_N V_D}{(N+h)^2} - \dfrac{V_E V_N \tan(\phi)}{(N+h)^2} \\ 2V_E\omega_e \sin(\phi) & 0 & \dfrac{V_E^2}{(N+h)} + \dfrac{V_N^2}{(M+h)} - \dfrac{2\gamma}{(R+h)} \end{bmatrix} \quad \text{(A.3)}$$

$$F_{vv} = \begin{bmatrix} \frac{V_D}{(M+h)} & -2\omega_e \sin(\phi) - \frac{2V_E \tan(\phi)}{(N+h)} & \frac{V_N}{(M+h)} \\ 2\omega_e \sin(\phi) + \frac{V_E \tan(\phi)}{(N+h)} & \frac{V_D + V_N \tan(\phi)}{(N+h)} & 2\omega_e \cos(\phi) + \frac{2V_E}{(N+h)} \\ -\frac{2V_N}{(M+h)} & -2\omega_e \cos(\phi) - \frac{2V_E}{(N+h)} & 0 \end{bmatrix} \quad \text{(A.4)}$$

$$F_{\varepsilon r} = \begin{bmatrix} -\omega_e \sin(\phi) & 0 & \frac{-V_E}{(N+h)^2} \\ 0 & 0 & \frac{V_N}{(M+h)^2} \\ -\omega_e \cos(\phi) - \frac{V_E}{(N+h)\cos^2(\phi)} & 0 & \frac{V_E \tan(\phi)}{(N+h)^2} \end{bmatrix} \quad \text{(A.5)}$$

$$F_{\varepsilon v} = \begin{bmatrix} 0 & \frac{1}{(N+h)} & 0 \\ -\frac{1}{(M+h)} & 0 & 0 \\ 0 & \frac{-\tan(\phi)}{(N+h)} & 0 \end{bmatrix} \quad \text{(A.6)}$$

$$F_{\varepsilon\varepsilon} = \begin{bmatrix} 0 & \omega_e \sin(\phi) + \frac{V_E \tan(\phi)}{(N+h)} & \frac{V_N}{(M+h)} \\ -\omega_e \sin(\phi) - \frac{V_E \tan(\phi)}{(N+h)} & 0 & -\omega_e \cos(\phi) - \frac{V_E}{(N+h)} \\ -\omega_e \cos(\phi) - \frac{V_E}{(N+h)\cos^2(\phi)} & \omega_e \cos(\phi) + \frac{V_E}{(N+h)} & 0 \end{bmatrix} \quad \text{(A.7)}$$

where $v^n \triangleq \begin{bmatrix} v_N & v_E & v_D \end{bmatrix}^T$ is the velocity vector in the n-frame and the rest of the parameters were defined in the text.